

Theoretical Model for the Superconducting and Magnetically Ordered Borocarbides

A. Amici,¹ P. Thalmeier,² and P. Fulde¹

¹Max-Planck-Institut für Physik komplexer Systeme, D-01187 Dresden, Germany

²Max-Planck-Institut für Chemische Physik fester Stoffe, D-01187 Dresden, Germany

(Received 28 May 1999)

We present a theory of superconductivity in the presence of a general magnetic structure in a form suitable for the description of complex magnetic phases encountered in borocarbides. The theory, complemented with some details of the band structure and with the magnetic phase diagram, may explain the nearly reentrant behavior and the anisotropy of the upper critical field of $\text{HoNi}_2\text{B}_2\text{C}$. The onset of the helical magnetic order depresses superconductivity via the reduction of the interaction between phonons and electrons caused by the formation of magnetic Bloch states. At mean field level, no additional suppression of superconductivity is introduced by the incommensurability of the helical phase.

PACS numbers: 74.70.Dd, 74.25.Dw, 74.25.Ha

In 1957 Ginzburg first showed that superconductivity and long range ferromagnetic order compete with each other, making their mutual coexistence nearly impossible [1]. On the other hand, in 1963 Baltensperger and Strässler pointed out that in the case of antiferromagnetic order the two order parameters may actually coexist [2]. Two families of magnetically ordered superconductors, the rare earth ternary compounds RRh_4B_4 and RMO_6S_8 , were almost simultaneously discovered in the late 1970s and both theoretical predictions proved to be correct; see, e.g., Ref. [3] for an extensive review.

More recently the discovery of quaternary compounds of the family $\text{RNi}_2\text{B}_2\text{C}$, with $R = \text{Lu}, \text{Y}$, or rare earth element [4,5], renewed the interest in the issue because more complex magnetic structures were observed to coexist or to compete with superconductivity (for a review see Ref. [6]). For $R = \text{Er}$ and Tm the magnetic structures coexisting with superconductivity are incommensurate transversely polarized spin-density waves: $T_c = 11 \text{ K}$ and $T_N = 6.8 \text{ K}$ for Er and $T_c = 11 \text{ K}$ and $T_N = 1.5 \text{ K}$ for Tm . $\text{DyNi}_2\text{B}_2\text{C}$, with $T_c = 6 \text{ K}$, orders in a commensurate antiferromagnetic state at $T_N = 10.6 \text{ K}$ and it is the only borocarbide compound with $T_N > T_c$. The case of $\text{HoNi}_2\text{B}_2\text{C}$ ($T_c = 8\text{--}9 \text{ K}$) is more complex: The transitions into two incommensurate magnetically ordered states, at $T_{\text{IC}}^c \approx T_{\text{IC}}^a \approx 6 \text{ K}$ with wave vectors $\mathbf{Q}_c = 0.91\mathbf{c}^*$ and $\mathbf{Q}_a = 0.55\mathbf{a}^*$, respectively, coincide with a deep depression of the superconducting upper critical field [7], while below the transition temperature $T_N \approx 5 \text{ K}$ into a commensurate antiferromagnetic state, with $\mathbf{Q}_{\text{AF}} = \mathbf{c}^*$, H_{c2} rapidly recovers. The anisotropic upper-critical-field phase diagram with the magnetic field along the symmetry directions of the crystal is given in Ref. [8]. Experimental data on pseudoquaternary borocarbides [9,10] add insight on the dramatic effects that the presence of magnetic order produces on superconductivity. On the other hand, no difference is found in the magnetic properties of related superconducting and nonsuperconducting compounds.

Borocarbides have a body-centered-tetragonal lattice structure with $I4/mmm$ space group symmetry. In spite of their layered structure they possess three-dimensional conduction bands of mainly Ni $3d$ character [11,12]. The strongly anisotropic magnetic properties are associated with the localized $4f$ electrons of the rare earths. The two types of electrons interact weakly via the local spin exchange on the rare earth sites. Relying on experimental evidence we consider the $4f$ -electron system to be independent from the state (normal or superconducting) of the conduction electrons. Theoretically this is justified by the separation in the energy scales associated with the two ordering phenomena: $E_{\text{MO}} \sim k_B T_M$ for magnetic order and $E_{\text{SC}} \sim (k_B T_c)^2 / E_F$ for the superconductivity. Careful treatment is needed for magnetic structures with small \mathbf{q} (e.g., $|\mathbf{q}| < 1/\xi$, with ξ the coherence length) or originating from nesting features of the Fermi surface. In fact, the opening of the small superconducting gap affects significantly the RKKY-type magnetic interaction in the regions of \mathbf{q} space close to zero or to a nesting vector. However, away from these special \mathbf{q} points, the structure of the magnetic interaction is related to electron-hole excitations of all energies and is independent from the presence of superconductivity. Therefore, it is possible to take the magnetic properties of borocarbides from experiments or from an independent microscopic magnetic model and concentrate on the influence which the molecular field of the ordered moments has on the conducting electrons. Similar approaches have been used in the cases of the antiferromagnetic [13,14] and small \mathbf{q} helical order [15] coexisting with superconductivity in RRh_4B_4 and RMO_6S_8 . More recently the same technique has been used for a qualitative discussion of the properties of $\text{HoNi}_2\text{B}_2\text{C}$ [16,17].

The aim of this Letter is to present a theory of superconductivity in an arbitrarily modulated exchange field capable of describing the magnetic structures encountered in the borocarbides. Applied to the upper-critical-field phase diagram of $\text{HoNi}_2\text{B}_2\text{C}$, the theory reproduces naturally its

several anomalous features and gives an explanation for its nearly reentrant behavior.

We introduce the following BCS model Hamiltonian for the conduction electrons in the presence of a periodic molecular field:

$$\mathcal{H} = \mathcal{H}_b + \mathcal{H}_{b-4f} + \mathcal{H}_{b-b}, \quad (1)$$

$$\mathcal{H}_b = \sum_k \epsilon_{\mathbf{k}} c_k^\dagger c_k, \quad (2)$$

$$\mathcal{H}_{b-4f} = \sum_{\mathbf{q}} I(\mathbf{q}) \langle \mathbf{S}_{\mathbf{q}} \rangle \cdot \mathbf{s}_{\mathbf{q}}, \quad (3)$$

$$\mathcal{H}_{b-b} = \frac{1}{2} \sum_{k'_1 k'_2 k_1} V_{k'_2 k'_1}^{k_2 k_1} c_{k'_1}^\dagger c_{k'_2}^\dagger c_{k_2} c_{k_1}. \quad (4)$$

The term \mathcal{H}_b is the Hamiltonian for the free conduction band electrons, and c_k^\dagger ($= c_{\mathbf{k}\sigma}^\dagger$) and c_k ($= c_{\mathbf{k}\sigma}$) are, respectively, the creation and annihilation operators for a state with quantum number $k = (\mathbf{k}, \sigma)$. The term \mathcal{H}_{b-4f} is the exchange interaction between the spin of the local 4f moments $\langle \mathbf{S}_{\mathbf{R}_i} \rangle$ (with Fourier transform $\langle \mathbf{S}_{\mathbf{q}} \rangle$) and the spin of the conduction electrons, $\mathbf{s}_{\mathbf{q}} = \sum_{\mathbf{k}\sigma\sigma'} c_{\mathbf{k}+\mathbf{q}\sigma'}^\dagger \boldsymbol{\sigma}_{\sigma'\sigma} c_{\mathbf{k}\sigma}$. At the moment we do not specify any magnetic configuration and we require only the periodicity of the known function $\langle \mathbf{S}_{\mathbf{R}_i} \rangle$. \mathcal{H}_{b-b} is the intraband interaction term whose attractive part leads to superconductivity. Note that $V_{k'_2 k'_1}^{k_2 k_1} = 0$ for all matrix elements not conserving spin and crystal momentum (in the form $\mathbf{k}'_2 + \mathbf{k}'_1 + \mathbf{G} = \mathbf{k}_2 + \mathbf{k}_1$, with \mathbf{G} a reciprocal lattice vector).

The first two terms of the total Hamiltonian are bilinear and therefore may be easily diagonalized for the magnetic structures encountered in the borocarbides (i.e., helices and spin-density waves). The magnetic Bloch states obtained this way, with creation and annihilation operators \tilde{c}_k^\dagger ($= \tilde{c}_{\mathbf{k}\tau}^\dagger$) and \tilde{c}_k ($= \tilde{c}_{\mathbf{k}\tau}$), are labeled by the momentum \mathbf{k} and the quantum number $\tau = +$ or $-$. As a convention we assume the momentum \mathbf{k} to belong to the nonmagnetic Brillouin zone, in order not to introduce an additional magnetic band index. Correspondingly the law of crystal momentum conservation is satisfied modulo a vector in the magnetic reciprocal lattice $\tilde{\mathbf{G}}$. The magnetic reciprocal lattice may be constructed by adding to every nonmagnetic vector \mathbf{G} a finite set of vectors $\{\mathbf{G}^M\}$, and momentum conservation requires $\mathbf{k}'_2 + \mathbf{k}'_1 + \mathbf{G} + \mathbf{G}^M = \mathbf{k}_2 + \mathbf{k}_1$. In the new basis the Hamiltonian (1) reduces to $\tilde{\mathcal{H}} = \tilde{\mathcal{H}}_b + \tilde{\mathcal{H}}_{b-b}$ with $\tilde{\mathcal{H}}_b$ and $\tilde{\mathcal{H}}_{b-b}$ given by Eqs. (2) and (4) with all the symbols written with tildes. When spin degeneracy is lifted, the energy $\epsilon_{\mathbf{k}}$ becomes $\tilde{\epsilon}_k$. Now the Hamiltonian $\tilde{\mathcal{H}}$ is formally very similar to the usual BCS Hamiltonian. The main differences are the modified law of the momentum conservation and the additional \mathbf{k} dependence of the magnetic energy bands $\tilde{\epsilon}_k$ and the electron-electron interaction $\tilde{V}_{k'_2 k'_1}^{k_2 k_1}$. The mean field approximation may be

applied to $\tilde{\mathcal{H}}$ in the same way as in the nonmagnetic case, via the introduction of the gap functions of the new magnetic eigenstates $\Delta_{\mathbf{G}^M}^{\tau\tau}(\mathbf{k})$ corresponding to the anomalous Green functions $\langle \tilde{c}_{-\mathbf{k}+\mathbf{G}^M\tau'} \tilde{c}_{\mathbf{k}\tau} \rangle$. The function $\Delta_{\mathbf{G}^M}^{\tau\tau}(\mathbf{k})$ is actually a matrix in the τ indices in order to include odd and even parities.

Some general qualitative properties of the magnetic Bloch states and the implications of their use for superconductivity have been discussed in Ref. [18]. However, numerical complications due to the nontrivial \mathbf{k} dependence introduced so far prevent the solution of the self-consistent gap equations in the general case. In order to proceed further the explicit form of the underlying magnetic structure of a particular material is needed.

The obvious choice for the first application of this formalism is the analysis of the much debated issue of the almost reentrant upper critical field in $\text{HoNi}_2\text{B}_2\text{C}$. In what follows we concentrate on the magnetic ordered states with periodicity along the c axis: the high temperature incommensurate helix ($\mathbf{Q}_c = 0.91\mathbf{c}^*$) and the low temperature commensurate antiferromagnetic state ($\mathbf{Q}_{\text{AF}} = \mathbf{c}^*$). The qualitative features of the lock-in transition are reproduced by theoretical model including the RKKY interaction and the crystalline electric field (CEF). Two such models [19,20] were first developed to account for the complex meta-magnetic phase diagram of $\text{HoNi}_2\text{B}_2\text{C}$ at $T = 2$ K [21]. In particular, the model in Ref. [19], which includes the actual CEF states of Ho, is capable to produce a temperature dependent phase diagram, which is used here as input. All the parameters of this model have been fitted to the low temperature magnetic properties of the normal state [19] and are not considered adjustable quantities in what follows. In Fig. 1 we show the magnetic phase diagram of the model as a function of the temperature and of the magnetic field along the easy axis of the Ho moments, given by the crystallographic $\langle 110 \rangle$ direction.

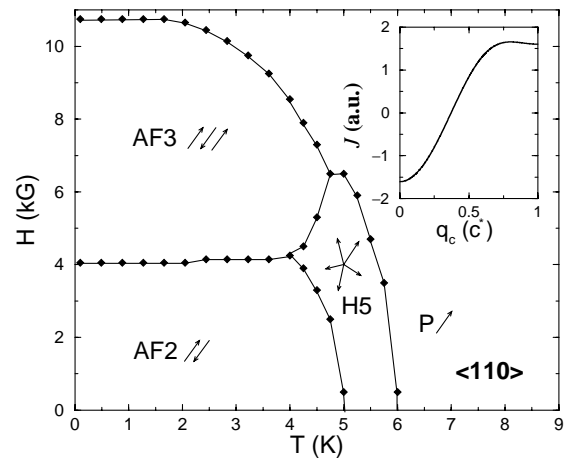


FIG. 1. Magnetic phase diagram for $\text{HoNi}_2\text{B}_2\text{C}$ in the H - T plane obtained from the model discussed in Ref. [19]. The magnetic field lies along the $\langle 110 \rangle$ easy direction (\nearrow). The phases have ferromagnetic alignment in the ab plane and the stacking sequences along the c axis shown in the figure. Inset: The RKKY interaction function $J(\mathbf{q})$.

Input data for the coexistence analysis are the following calculated quantities: the underlying magnetic structure, the temperature dependent magnetic order parameter $S(T)$, the magnetic energies, and the magnetic susceptibility.

Given the helical magnetic structure $\mathbf{S}_{\mathbf{R}_i} = S[\hat{\mathbf{a}} \cos(\mathbf{Q} \cdot \mathbf{R}_i) + \hat{\mathbf{b}} \sin(\mathbf{Q} \cdot \mathbf{R}_i)]$, the interaction Hamiltonian in Eq. (3) has the following explicit form:

$$\mathcal{H}_{b-4f} = IS \sum_{\mathbf{k}\sigma\sigma'} (c_{\mathbf{k}-\mathbf{Q}\sigma'}^+ \sigma_{\sigma'\sigma}^+ c_{\mathbf{k}\sigma} + c_{\mathbf{k}+\mathbf{Q}\sigma'}^+ \sigma_{\sigma'\sigma}^- c_{\mathbf{k}\sigma}) \quad (5)$$

with $\sigma^\pm = \sigma_x \pm i\sigma_y$. The corresponding magnetic states are found via simple Bogoliubov transformation of the type $\tilde{c}_{\mathbf{k}\uparrow}^+ = u_{\mathbf{k}} c_{\mathbf{k}\uparrow}^+ + v_{\mathbf{k}} c_{\mathbf{k}+\mathbf{Q}\downarrow}$ where the state (\mathbf{k}, \uparrow) mixes with only one other state, namely $(\mathbf{k} + \mathbf{Q}, \downarrow)$, independently of the value of \mathbf{Q} [22]. The Bogoliubov coefficients $u_{\mathbf{k}}$ and $v_{\mathbf{k}}$, the new energies $\tilde{\epsilon}_{\mathbf{k}}$, and the new scattering matrix can be derived analytically in close analogy with the antiferromagnetic case. In particular, we have

$$u_{\mathbf{k}}^2 - v_{\mathbf{k}}^2 = \sqrt{\frac{(\epsilon_{\mathbf{k}} - \epsilon_{\mathbf{k}+\mathbf{Q}})^2}{(\epsilon_{\mathbf{k}} - \epsilon_{\mathbf{k}+\mathbf{Q}})^2 + 4I^2S^2}} \quad (6)$$

and

$$\tilde{\epsilon}_{\mathbf{k}\pm} = \frac{\epsilon_{\mathbf{k}} + \epsilon_{\mathbf{k}\pm\mathbf{Q}}}{2} + \frac{\epsilon_{\mathbf{k}} - \epsilon_{\mathbf{k}\pm\mathbf{Q}}}{2} \times \sqrt{1 + \frac{4I^2S^2}{(\epsilon_{\mathbf{k}} - \epsilon_{\mathbf{k}\pm\mathbf{Q}})^2}}. \quad (7)$$

The expression for $\tilde{v}_{k_2 k_1}^{k_2 k_1}$ (not shown) is analytic as well. However, even assuming the simple BCS interaction potential in the nonmagnetic state, it is rather complicated. It is important to note that the magnetic energy bands $\tilde{\epsilon}_{\mathbf{k}}$ possess magnetic gaps for only the two pairs of magnetic-Bragg planes orthogonal to the c axis at distances $Q/2$ and $(c^* - Q/2)$ from the Γ point and that all the magnetic quantities differ from the nonmagnetic ones only in narrow regions around these planes [22]. The presence of only four active magnetic-Bragg planes for any commensurate value of the ordering vector \mathbf{Q} make the following arguments hold for structures with arbitrary periodicity. If we assume that the onset of magnetic order affects the superconducting state as a perturbation, the only sizable components of the gap function matrix are $\Delta_0^{+-} = -\Delta_0^{-+} \equiv \Delta$ [17]. After some algebraic manipulations the gap equation simplifies considerably and the gap function may be written as $\Delta(\mathbf{k}, T) = (u_{\mathbf{k}}^2 - v_{\mathbf{k}}^2)\Delta(T)$ [17]. This leads to

$$\Delta(T) = \int_0^{\omega_D} d\epsilon \left(V \int_{\text{MFS}} \frac{dS'}{(2\pi)^3} \frac{(u_{\mathbf{k}'}^2 - v_{\mathbf{k}'}^2)^2}{|\nabla_{\mathbf{k}'} \tilde{\epsilon}_{\mathbf{k}'}|} \right) \times \frac{\Delta(T)\mathcal{F}(T)}{\sqrt{\epsilon^2 + \Delta^2(T)}}, \quad (8)$$

where $\mathcal{F}(T) \equiv (1 - 2n_{\mathbf{k}'})$ takes into account the occupation of the electronic states and we have approximated $\Delta(\mathbf{k}, T)$ with $\Delta(T)$ in the square root. Equation (8) corresponds to the usual BCS self-consistent equation with an effective interaction parameter $\lambda_e(T)$ defined as the term into brackets. $\lambda_e(T)$ depends on the underlying magnetic state through the Bogoliubov coefficients and through the shape of the magnetic Fermi surface (MFS). Since all the anomalous magnetic \mathbf{k} dependencies come from the regions where the Fermi surface intersects the four Bragg planes, the difference $\Delta\lambda(T) = \lambda - \lambda_e(T)$ between the actual electron-phonon interaction parameter (λ) and the effective one may be expanded in terms of $\frac{IS(T)}{\epsilon_F}$. This simplifies considerably the analysis because only very limited knowledge of the actual band structure is needed in order to estimate the variation $\Delta\lambda(T)$ of the effective interaction. Therefore the high temperature interaction parameter λ can be considered a phenomenological parameter to be determined by the transition temperature T_c . An inspection of the local-density approximation (LDA) band structure of $\text{HoNi}_2\text{B}_2\text{C}$ [23] suggests approximate rotational symmetry at the intersection between the Fermi surface and the Bragg planes corresponding to the observed magnetic phases. With the assumption of rotational symmetry the only parameters we need for the band structure are the radial and vertical components of the Fermi velocity v_r, v_z at the intersections. To first order in the parameter $\frac{IS(T)}{\epsilon_F}$, for the two pairs of Bragg planes we have

$$\Delta\lambda(T) = -\frac{V}{2\pi\hbar^2} \frac{k_r}{v_r v_z} IS(T), \quad (9)$$

where k_r is the radius of the intersection. We note that the two components of the Fermi velocity enter Eq. (9) independently and the perturbation expansion actually breaks down if v_r or v_z are much smaller than v_F . In particular, in the case of nesting we have $v_r \ll v_F$ and $\Delta\lambda(T)$ is not a linear function of $S(T)$. However, the magnetic structures along the c axis are not linked to nesting and may safely be treated within our perturbation expansion. We assume the relevant phonons to have an average energy $\omega_D = 40$ meV and with the value $T_c = 8.5$ K, the BCS formula gives us a value of $\lambda = 0.25$. Taking into account the closeness of the two magnetic ordering vectors $Q_{\text{AF}} = \mathbf{c}^*$ and $Q_c = 0.91\mathbf{c}^*$ we assume v_r, v_z , and k_r not to change with the lock-in. This means that we treat the incommensurate and the commensurate phases exactly on the same footing.

The main features of the experimental anisotropic phase diagram of $\text{HoNi}_2\text{B}_2\text{C}$ are reported in Ref. [8] which we will use in order to compare our results. The upper critical field may be calculated from the equation

$$H_{c2}^{(110)}(T) = B_{c2}^{\text{BCS}}(\lambda(T), T) - M(T), \quad (10)$$

where $B_{c2}^{\text{BCS}}(\lambda(T), T)$ is the critical field value in the nonmagnetic BCS case and $M(T)$ is the magnetization in the normal state. Since the magnetic response of $\text{HoNi}_2\text{B}_2\text{C}$ is very weak along the c axis, we may neglect the

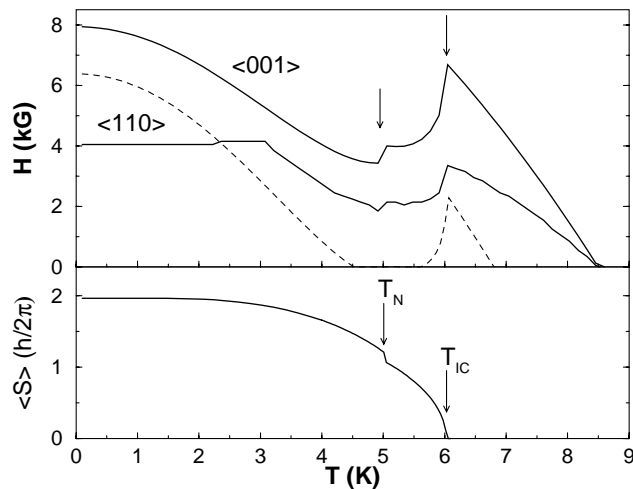


FIG. 2. Lower panel: Size of the magnetic order parameter $\langle S \rangle$ vs temperature. For temperatures above (below) the first order lock-in transition temperature T_N the H5 (AF2) order parameter is plotted. Upper panel: Upper critical field curves $H_{c2}(T)$ along the $\langle 001 \rangle$ and the $\langle 110 \rangle$ directions. The dashed line is the $\langle 001 \rangle$ curve with T_c reduced to 6.8 K.

magnetization term, and the upper critical field curve that we obtain is the upper line ($\langle 001 \rangle$) in Fig. 2 where we have used the value for $\Delta\lambda(0K)/\lambda = 0.12$. The depression of the critical field is then due to the onset of the magnetic order altogether and not to its incommensurate nature. The depression results from a small but rapid decrease of the effective interaction parameter $\lambda_e(T)$ related to any helical structure, regardless of its periodicity. Furthermore, the almost reentrant behavior shown in Fig. 2 is produced by a reduction in the value of λ by only 12%. The small jump at the lock-in transition is due to the discontinuity of the single-site magnetization going from five-cell helix to the antiferromagnet shown in the lower part of Fig. 2.

In order to reproduce the other features of the anisotropic upper critical field phase diagram it is important to take into account the strong anisotropic magnetic response of the system and the presence of meta-magnetic transitions in the same range of fields and temperatures. In Fig. 2 is shown the curve for the external field along the $\langle 110 \rangle$ direction calculated with the $M(T)$ response of the magnetic system. With respect to the $\langle 001 \rangle$ curve, the peak around 6 K is strongly reduced by the magnetization, while for temperatures below 4 K the two curves approach each other due to the saturation of the ordered microscopic magnetic moments and the subsequently reduced magnetic response of the system. The low temperature plateau is due to the transition to the meta-magnetic phase AF3 (compare with Fig. 1) which has a large ferromagnetic component and suppresses superconductivity much more strongly than the low field antiferromagnet. The $\langle 100 \rangle$ critical field curve (not shown) has almost the same shape as the $\langle 110 \rangle$ curve for temperatures higher than 3 K, but the plateau is reached at a slightly smaller temperature and for a slightly larger value of the magnetic field. This corresponds to the upper shift of the meta-magnetic transition to AF3. All

these features are in quantitative agreement with the experimental data [8].

In addition, our model explains in a natural way the fact that $\text{HoNi}_2\text{B}_2\text{C}$ samples with T_c reduced via different techniques, i.e., with Co doping [10], actually reenter the normal state in a temperature region around the lock-in transition T_N . The dashed line in Fig. 2 is the upper critical field along the c axis obtained leaving all the parameters except T_c unchanged.

In conclusion, we derived a theory of superconductivity in a magnetically ordered background, and we applied it to the case of $\text{HoNi}_2\text{B}_2\text{C}$. We interpreted the main anomaly of its upper critical field via the reduction of the interaction between phonons and electrons in the Bloch states of the magnetic structure. In this respect, the effect of a helical magnetic background on superconductivity is identical to the effect of antiferromagnetism. The helical case can be treated analytically independently of the periodicity and the incommensurate limit does not introduce additional suppression. Finally, the anisotropy of the magnetic field and the temperature phase diagram are well reproduced by taking into account the magnetic response of the material.

We thank H. Rosner for the data on the LDA band structure of $\text{HoNi}_2\text{B}_2\text{C}$. This work was performed under DFG Sonderforschungsbereich 463.

- [1] V.L. Ginzburg, Sov. Phys. JETP **4**, 153 (1957).
- [2] W. Baltensperger and S. Strässler, Z. Phys. B **1**, 20 (1963).
- [3] *Superconductivity in Ternary Compounds*, edited by M.B. Maple and Ø. Fischer (Springer-Verlag, Berlin, 1982), Vols. I & II.
- [4] R. Nagarajan *et al.*, Phys. Rev. Lett. **72**, 274 (1994).
- [5] R.J. Cava *et al.*, Nature (London) **367**, 252 (1994).
- [6] J.W. Lynn *et al.*, Phys. Rev. B **55**, 6584 (1997).
- [7] H. Eisaki *et al.*, Phys. Rev. B **50**, 647 (1994).
- [8] K. Krug, M. Heinecke, and K. Winzer, Physica (Amsterdam) **267C**, 321 (1996).
- [9] B.K. Cho, P.C. Canfield, and D.C. Johnston, Phys. Rev. Lett. **77**, 163 (1996).
- [10] H. Schmidt and H.F. Braun, Phys. Rev. B **55**, 8497 (1997).
- [11] L.F. Mattheiss, Phys. Rev. B **49**, 13279 (1994).
- [12] W.E. Pickett and D.J. Singh, Phys. Rev. Lett. **72**, 3702 (1994).
- [13] A.I. Morozov, Sov. Phys. Solid State **22**, 1974 (1980).
- [14] G. Zwirgagl and P. Fulde, Z. Phys. B **43**, 23 (1981).
- [15] A.I. Morozov and L.V. Panina, Sov. Phys. Solid State **23**, 769 (1981).
- [16] A.I. Morozov, JETP Lett. **63**, 734 (1996).
- [17] A.I. Morozov, Sov. Phys. JETP **83**, 1048 (1996).
- [18] A. Amici, P. Thalmeier, and P. Fulde, Physica (Amsterdam) **317-318C**, 471 (1999).
- [19] A. Amici and P. Thalmeier, Phys. Rev. B **57**, 10684 (1998).
- [20] V.A. Kalatsky and V.L. Pokrovsky, Phys. Rev. B **57**, 5485 (1998).
- [21] P.C. Canfield *et al.*, Phys. Rev. B **55**, 970 (1997).
- [22] C. Herring, in *Magnetism, Vol. IV*, edited by G.T. Rado and H. Suhl (Academic Press, New York, 1966), pp. 303–315.
- [23] S.-L. Drechsler *et al.*, Physica (Amsterdam) **317-318C**, 117 (1999).